Novel Urchin-like CuO Synthesized by a Facile Reflux Method with Efficient Olefin Epoxidation Catalytic Performance

Linping Xu,[†] Shanthakumar Sithambaram,[†] Yashan Zhang,[†] Chun-Hu Chen,[†] Lei Jin,[†] Raymond Joesten,[†] and Steven L. Suib*[,†,‡]

Department of Chemistry, U-3060, and Institute of Materials Science, U-3136, University of Connecticut, Storrs, Connecticut 06269

Received October 24, 2008. Revised Manuscript Received February 5, 2009

CuO is an important transition metal oxide with a narrow bandgap ($E_g = 1.2$ eV). CuO has been used as a catalyst, a gas sensor, in anode materials for Li ion batteries. CuO has also been used to prepare high temperature superconductors and magnetoresistance materials. In this paper, CuO with urchin-like morphologies has been synthesized via a simple reflux method. The reflux method has advantages over other solution-based techniques, such as ease of operation, safety, and high yield (95%). XRD results showed pure tenorite CuO was produced. FE-SEM exhibited an urchin-like morphology of CuO, which is composed of aggregates of nanosized strips. HR-TEM showed that the strips were single crystals with the lattice fringe of 2.3 Å, which corresponds to (111). DSC and TGA results suggested that as-synthesized CuO had high thermal stability. Time-dependent experiments were conducted to illustrate the evolution of the urchin-like morphology and crystal phase formation of CuO. The effects of copper sources and precipitators on the phase and morphology of the products were studied. As-synthesized CuO showed much better catalytic performance, increased yield (from 64.3% to 89.5%) for olefin epoxidation than commercial CuO and CuO prepared by thermal decomposition of copper hydroxide.

1. Introduction

Control of the shapes and structures of transition metal oxides has attracted significant interest in materials syntheses.[1−10] The optical and electrical properties and catalytic performance of the materials are strongly influenced by the morphologies and crystallographic forms.[1−5,10,11] Many investigations have been made to study the self-assembly of one-dimensional (1D) wires or rods into two-dimensional (2D) and three-dimensional (3D) hierarchical structures.[12−14] However, it is challenging to develop an easier-to-operate, template-free, solution-based, and morphology-controllable approach to fabricate novel self-generated architectures.

CuO is an interesting transition metal oxide with a narrow band gap ($E_g = 1.2$ eV) and has been recognized as being used in preparing high temperature superconductors and magnetoresistance materials.[15] CuO is also a promising catalyst and support in many organic reactions.[16−20] CuO crystalline material also could be used as anode materials for Li ion batteries. Copper oxide materials have been of considerable interest as they have been found to be effective catalysts for CO and NO oxidation as well as oxidation of volatile organic chemicals such as methanol.[21] Recently, C−N coupling reactions also have been reported using nanocrystalline CuO as a catalyst with excellent activities.[22] Rout et al. have reported an efficient CuO catalyzed C−S cross-coupling of thiols with iodobenzene.[23] Therefore, the synthesis and the application study of CuO have both theoretical and practical importance.

* To whom correspondence should be addressed. E-mail: steven.suib@uconn.edu.
[†] Department of Chemistry, University of Connecticut.
[‡] Institute of Materials Science, University of Connecticut.

(1) Liu, J.; Huang, X.; Li, Y.; Sulieman, K. M.; He, X.; Sun, F. *Cryst. Growth Des.* **2006**, *6*, 16901.
(2) Zhang, J.; Liu, J.; Peng, Q.; Wang, X.; Li, Y. *Chem. Mater.* **2006**, *18*, 867.
(3) Xiao, H.-M.; Fu, S.-Y.; Zhu, L.-P.; Li, Y.-Q.; Yang, G. *Eur. J. Inorg. Chem.* **2007**, 1966.
(4) Xu, Y.; Chen, D.; Jiao, X. *J. Phys. Chem. B* **2005**, *109*, 13561.
(5) Gao, X. P.; Bao, J. L.; Pan, G. L.; Zhu, H. Y.; Huang, P. X.; Wu, F.; Song, D. Y. *J. Phys. Chem. B* **2004**, *108*, 5547.
(6) Liu, B.; Zeng, H. C. *J. Am. Chem. Soc.* **2004**, *126*, 8124.
(7) Yu, H.; Yu, J.; Liu, S.; Mann, S. *Chem. Mater.* **2007**, *19*, 4327.
(8) Wang, X.; Xi, G.; Xiong, S.; Liu, Y.; Xi, B.; Yu, W.; Qian, Y. *Cryst. Growth Des.* **2007**, *7*, 930.
(9) Xu, Y.; Chen, D.; Jiao, X.; Xue, K. *Mater. Res. Bull.* **2007**, *42*, 1723.
(10) Zhao, Y.; Zhu, J.-J.; Hong, J.-M.; Bian, N.; Chen, H.-Y. *Eur. J. Inorg. Chem.* **2004**, 4072.
(11) Xu, L.; Ding, Y.-S.; Chen, C.-H.; Zhao, L.; Rimkus, C.; Joesten, R.; Suib, S. L. *Chem. Mater.* **2008**, *20*, 308.
(12) Gu, Z.; Zhai, T.; Gao, B.; Sheng, X.; Wang, Y.; Fu, H.; Ma, Y.; Yao, J. *J. Phys. Chem. B* **2006**, *110*, 23829.
(13) Lu, F.; Cai, W.; Zhang, Y. *Adv. Funct. Mater.* **2008**, *18*, 1047.
(14) Zhang, T.; Dong, W.; Keeter-Brewer, M.; Sanjit, K.; Njabon, R. N.; Tian, Z. R. *J. Am. Chem. Soc.* **2006**, *128*, 10960.
(15) Wu, M. K.; Ashburn, J. R.; Torng, C. J.; Hor, P. H.; Meng, R. L.; Gao, L.; Huang, Z. J.; Wang, Y. Q.; Chu, C. W. *Phys. Rev. Lett.* **1987**, *58*, 908.
(16) Yin, G.; Zhou, B.; Meng, X.; Wu, A.; Pan, Y. *Org. Lett.* **2006**, *8*, 2245.
(17) Rout, L.; Jammi, S.; Punniyamurthy, T *Org. Lett.* **2007**, *9*, 3397.
(18) Rout, L.; Sen, T. K.; Punniyamurthy, T. *Angew. Chem., Int. Ed.* **2007**, *46*, 5583.
(19) Patil, N. S.; Uphade, B. S.; McCulloh, D. G.; Bhargava, S. K.; Choudhary, V. R. *Catal. Commun.* **2004**, *5*, 681.
(20) Thakuria, H.; Borah, B. M.; Das, G. *J. Mol. Catal. A: Chem.* **2007**, *274*, 1.
(21) Liu, Y.; Fu, Q.; Stephanopoulos; M, F. *Catal. Today* **2004**, *93−95*, 241.
(22) Kantam, M. L.; Yadav, J.; Laha, S.; Sreedhar, B.; Jha, S. *Adv. Synth. Catal.* **2007**, *349*, 1938.
(23) Jammi, S.; Sakthivel, S.; Rout, L.; Mukherjee, T.; Mandal, S.; Mitra, R.; Punniyamurthy, T. *J. Org. Chem.* **2009**, *74*, 1971.

10.1021/cm802915m CCC: $40.75
Published on Web 03/06/2009

CuO with different morphologies, such as nanoellipsoids,[1] nanoribbons,[8] nanorods,[3,5] nanotubes,[24] nanorings,[8] nanosphere,[2] nanocages,[25] hollow microsphere,[7] microflower,[9] aligned nanowires,[26] and dandelion,[6] have been successfully synthesized through different methods with or without the assistance of templates. Honeycomb and flowerlike CuO were fabricated by an anion-controlled self-assembly route, and the presence of WO_4^{2-} and MnO_4^{2-} helped in the construction of CuO nanoarchitectures on copper foils.[27] Hollow nanospheres of CuO were studied with the assistance of carbon spheres as hard templates.[28,29] In addition, template-directed synthesis was also applied for the formation of CuO nanotubes.[30] CuO with nanoribbons and nanorings morphologies were successfully obtained by the simple solution-phase reaction of $CuCl_2$ and NaOH with sodium dodecyl benzenesulfonate.[31] Thermal decomposition of copper oxalate was used to prepare nanosized CuO with optical and electrochemical properties.[32] Liu's group[6] studied the organization of nanoribbons to form dandelion-like CuO and discussed the mechanism of the formation process. Among all of these preparation methods, solution-based techniques showed special advantages for the generation of nanoarchitectures because of the mild synthesis conditions needed, potential for scale-up, economic factors, simpleness, and ease of operation. In these methods, hydrothermal methods were the most widely used one for fabrication of CuO with the kinds of morphologies reported in the literature. However, there are very few studies involving the fabrication of CuO using the reflux method. The reflux method even has advantages over hydrothermal methods, such as easy operation, safety, and high yield.

In this paper, we report a facile reflux method for the preparation of urchin-like CuO microspheres that involved organizing steps: (1) the formation of CuO strips from the flakelike copper nitrate hydroxide and (2) the self-assembly of CuO strips to urchin-like microspheres, which will then be used as the catalyst for olefin epoxidation.

Olefin epoxidation with peroxides involving heterogeneous catalysts is an alternative method compared with the traditional percarboxylic acids or the chlorohydrins route owing to the drawbacks from the latter, such as the use of corrosive conditions and production of toxic products. Titanium-based catalysts have been widely used for epoxidation.[33] However, these catalysts showed either poor activity or low selectivity for the epoxides. Supported gold catalysts showed improved activity;[19,34] however, the cost associated with gold catalysts, activity, the epoxide selectivity dependence on Au particle size, and the deactivation of catalysts in the presence of water are still challenging research problems. Many attempts have been made to overcome these drawbacks.[35−38] Most of the studies have focused on using transition metal oxides as catalysts for epoxidations instead of gold. However, the conversions and the selectivity obtained are not satisfactory. Urchin-like CuO materials prepared in this study not only improved the activity of epoxidation but are also compatible with water as a solvent.

2. Experimental Section

2.1. Synthesis of CuO. In a typical experiment, 10 mmol $Cu(NO_3)_2 \cdot 3H_2O$ and 50 mmol urea were dissolved in the solvent with 20 mL of distilled deionized water and 50 mL of ethylene glycol monomethyl ether in a round-bottom flask. After the clear blue solution was obtained, the magnetically stirred round-bottom flask with a water cooled condenser was transferred to an oil bath and the temperature of the oil bath was kept at 100 °C for 6 h. After the reaction, the products were transferred to a centrifuge tube immediately and washed in a centrifugation-redispersion cycle with distilled deionized water and ethanol several times, and dried in the oven at 80 °C overnight.

2.2. Characterization. *2.2.1. XRD.* The crystal structure of the sample was determined by X-ray diffraction (XRD) using a Scintag XDS 2000 diffractometer with Cu Kα radiation with a 1.5418 Å wavelength. A beam voltage of 45 kV and a 40 mA current beam were used. The CuO was further investgated by high-resolution transmission electron microscopy (HR-TEM). HRTEM studies were carried out on a JEOL 2010 instrument with an accelerating voltage of 200 kV. The samples for TEM were prepared by dispersing the material in 2-propanol by sonication. A drop of the dispersion was then placed on a carbon-coated gold grid and allowed to dry. Microdiffraction patterns (MDP), which are special convergent-beam electron diffraction (CBED), are obtained from HR-TEM to determine if the sample is single crystalline.

2.2.2. Morphology. Morphologies of the samples were investigated using a Zeiss DSM 982 Gemini field-emission scanning electron microscope (FE-SEM) with a Schottky emitter. Powder samples were dispersed in ethanol and dropped onto a gold-coated silicon wafer, and the wafer was then mounted onto a stainless steel sample holder using silver conductive paint. High resolution transmission electron microscopy (HR-TEM) was also used to check the morphologies of the samples. Energy-dispersive X-ray spectroscopy (EDX) was used for elemental analysis of the sample.

2.2.3. Surface Area and Porosity. N_2 physisorption was performed in a Micromeritics ASAP 2010 instrument to study surface area, pore volume, and pore size distribution of the CuO samples. Samples were pretreated by degassing at 120 °C overnight to remove any adsorbed species.

2.2.4. Thermal Stability. The thermal stability of the CuO materials was studied using simultaneous differential scanning calorimetry (DSC) and thermogravimetric analyses (TGA). DSC and TGA were performed on a Hi-Res TGA 2950 thermogravi-

(24) Cao, M.; Hu, C.; Wang, Y.; Guo, Y.; Guo, C.; Wang, E. *Chem. Commun* **2003**, 1884.
(25) Ng, C. H. B.; Fan, W. Y. *J. Phys. Chem. C* **2007**, *111*, 9166.
(26) Zhou, Y.; Kamiya, S.; Minamikawa, H.; Shimizu, T. *Adv. Mater.* **2007**, *19*, 4194.
(27) Liu, Y.; Chu, Y.; Zhuo, Y.; Li, M.; Li, L.; Dong, L. *Cryst. Growth Des.* **2007**, *7*, 467.
(28) Qian, H.; Lin, G.; Zhang, Y.; Gunawan, P.; Xu, R. *Nanotechnology* **2007**, *18*, 355602/1.
(29) Titirici, M.-M.; Antonietti, M.; Thomas, A. *Chem. Mater.* **2006**, *18*, 3808–3812.
(30) Bae, C.; Yoo, H.; Kim, S.; Lee, K.; Kim, J.; Sung, M. M.; Shin, H. *Chem. Mater.* **2008**, *20*, 756.
(31) Wang, X.; Xi, G.; Liu, Y.; Qian, Y. *Cryst. Growth Des.* **2008**, *8*, 1406.
(32) Zhang, X.; Zhang, D.; Ni, X.; Zheng, H. *Solid-State Electron.* **2008**, *52*, 245.
(33) Laha, S. C.; Kumar, R. *J. Catal.* **2001**, *204*, 64.
(34) Yin, D.; Qin, L.; Liu, J.; Li, C.; Jin, Y. *J. Mol. Catal. A: Chem.* **2005**, *240*, 40.
(35) Ghosh, R.; Shen, X.; Villegas, J. C.; Ding, Y.; Malinger, K.; Suib, S. L *J. Phys. Chem. B* **2006**, *110*, 7592.
(36) Choudhary, V. R.; Patil, N. S.; Chaudhari, N. K.; Bhargava, S. K. *J. Mol. Catal. A: Chem.* **2005**, *227*, 217.
(37) Sebastian, J.; Jinka, K. M.; Jasra, R. V. *J. Catal.* **2006**, *244*, 208.
(38) Jasra, R. V.; Sebastian, J. U.S. Patent Appl. US2007149791, June 28, 2007.

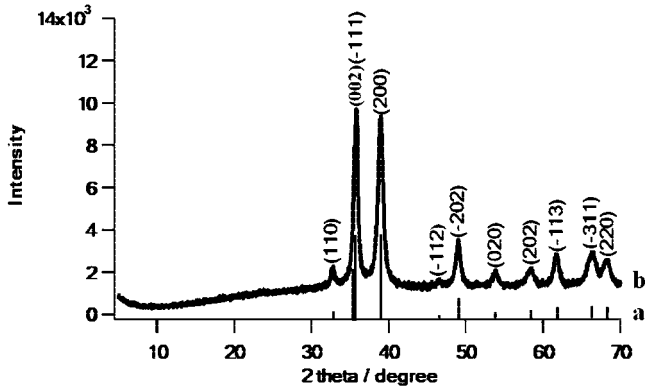

Figure 1. XRD pattern of CuO.

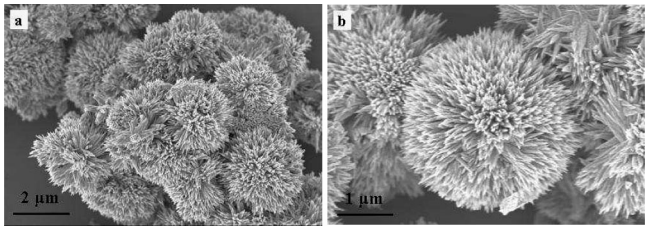

Figure 2. FE-SEM images of CuO.

metric analyzer with 60 mL/min of air or Ar flow from 25 to 700 °C at a heating rate of 10 °C/min.

2.2.5. Olefin Epoxidation. The epoxidation reactions were carried out in a batch reactor operating under reflux conditions at 70 °C for a period of 24 h. To a 50 mL round bottomed flask, 1 mmol of alkene, 10 mL of acetonitrile, and 10 mg of CuO catalyst were added. Finally, 5 mmol of TBHP was added dropwise to the mixture. The reaction mixture was continuously stirred using a magnetic stirrer. At the end of each reaction, aliquots were taken and diluted to constant concentration. Gas chromatography−mass spectroscopy (GC−MS) methods were used for identification and quantification. GC-MS analyses were done using an HP 5890 series II chromatograph with a thermal conductivity detector coupled with an HP 5970 mass selective detector. An HP-1 column (nonpolar cross-linked siloxane) with dimensions of 12.5 m × 0.2 mm × 0.33 μm was used in the gas chromatograph.

3. Results

3.1. XRD. X-ray diffraction (XRD) was used to study the phase purity of the obtained copper oxide, and the pattern is shown in Figure 1. The standard diffraction pattern for CuO was also shown for comparison, as shown in Figure 1a. All of the reflections in the XRD pattern in Figure 1b showed that tenorite CuO was obtained. No impurity peaks were observed. The XRD pattern agreed with the standard pattern (JCPDS 41−0254) in Figure 1a.

3.2. FE-SEM and HR-TEM. The morphology of CuO was studied by field emission scanning electron microscopy (FE-SEM) and high resolution transmission electron microscopy (HR-TEM). Figure 2 shows the SEM images of the as-obtained CuO, composed of urchin-like architectures with diameters of around 2 μm. A closer observation of the urchin-like morphology is shown in Figure 2b. The urchin-like architecture is composed of aggregates of strips. Figure 3a shows the HR-TEM images of CuO which are in good

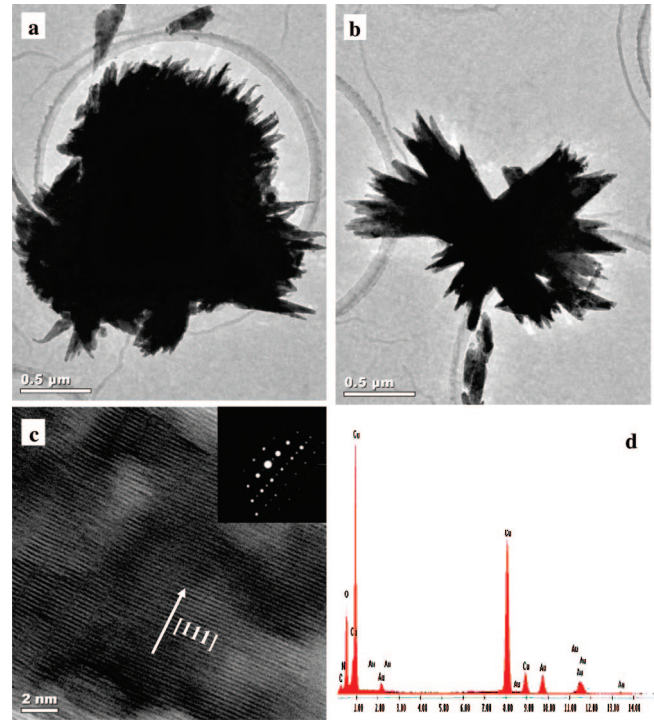

Figure 3. HR-TEM results and EDX of CuO.

agreement with the results from FE-SEM. Figure 3b is view of a broken urchin-like architecture. The lattice fringes of a strip with the lattice spacing of the (111) planes, $d \approx 2.3$ Å are shown in Figure 3c. The inset of the microdiffraction pattern (MDP) with beam direction of [1$\bar{1}$0] in Figure 3c suggests the single crystallinity of the strip. The energy dispersive X-ray spectroscopy (EDX) result showed that CuO was the only product, which was consistent with the XRD results.

3.3. Surface Area and Porosity. N_2 physisorption represents the most widely used technique to measure catalyst surface area and to study the texture of pores. The isotherm shape depends on the porous texture, composed of micropores, mesopores, and macropores. According to the IUPAC classification, six types of isotherms can be distinguished. Hysteresis is generated because during desorption, evaporation from mesopores usually takes place at a pressure lower than that of capillary condensation. The shape of the hysteresis loop is determined by the pore shapes. As for the CuO in this study, the isotherms of the adsorption cycles belonged to type II, which suggested macropores in the as-synthesized CuO, as shown in Figure 4. The hysteresis shape showed type H3, which means slit shaped pores were generated from the aggregates or agglomerates of particles. The inset in Figure 4 shows the pore size distribution calculated by the BJH method. Most of the pores were in the macropore range, which was consistent with the results from the shapes of isotherms. The specific surface area of urchin-like CuO is 15 m^2/g, and the pore volume is 0.04 cm^3/g.

3.4. Thermal Stability. The thermal stability of the as-synthesized CuO sample was studied by simultaneous DSC and TGA, which are used to characterize CuO in terms of a weight change or a phase change between 25 and 700 °C. The TGA and DSC curves of the CuO in air and in Ar are

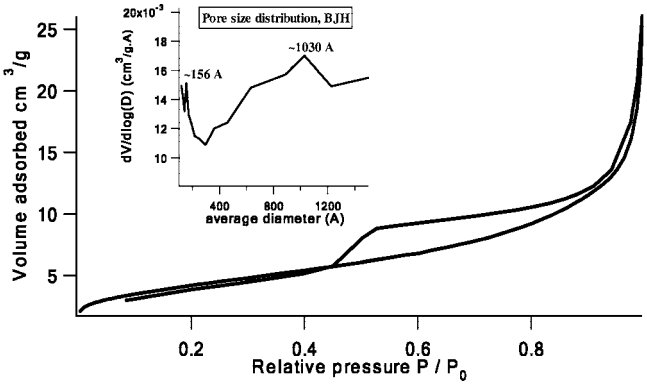

Figure 4. N_2 physisorption of CuO: absorption and desorption isotherms; inset is pore size distribution.

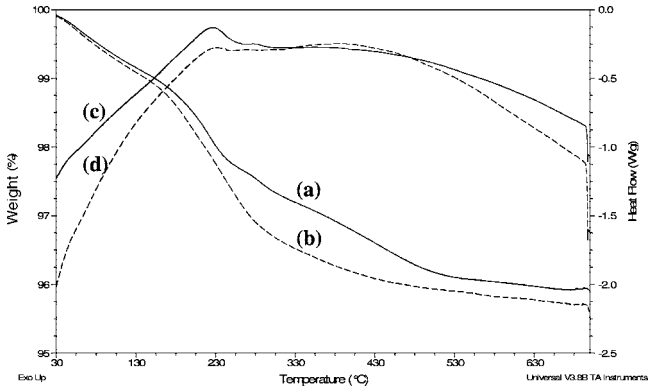

Figure 5. TGA and DSC plots of CuO in different atmospheres: (a, c) in air; (b, d) in Ar.

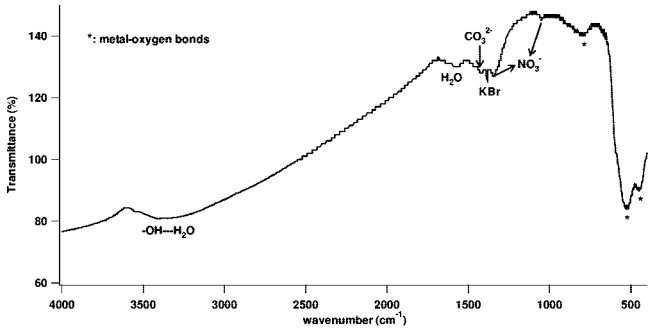

Figure 6. IR pattern of CuO.

shown in Figure 5. Either in air or in Ar atmosphere, there was not a large weight loss for CuO after heating to 700 °C. There was no sharp peak in the DSC curves, as shown in graphs c and d in Figure 5, which suggests that there was no change in the CuO during the heating process. Therefore, CuO in this study showed good thermal stability. XRD studies of the sample after thermal treatment showed no change in structure after heating to 700 °C.

Infrared spectra are used to detect the possible adsorbed species, as shown in Figure 6. The weight loss is carbonate ion, which is the byproduct from urea decomposition; nitrate ion, which is from the starting material; and adsorbed water.

3.5. Catalytic Studies. CuO materials have been reported to exhibit excellent catalytic activities in many applications of interest to the chemical industry. The catalytic activity of urchin-like CuO was evaluated for epoxidation of norbornene

Table 1. Epoxidation of Norbonene with Copper Oxide Catalysts[a]

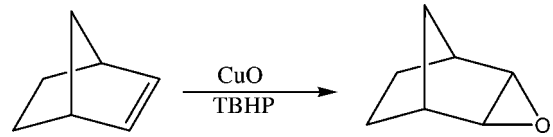

catalyst[b]	conversion (%)[c]	selectivity (%)[d]	TON[e]
CuO (1)	89.5	100	7.2
CuO (2)	78.3	100	6.2
CuO (3)[39]	64.3	100	5.8

[a] 1 mmol norbornene, 5 mmol TBHP, and 10.0 mg catalyst, stirred in 10 mL of actonitrile under reflux (70 °C) for 24 h. [b] (1) Urchin-like CuO, (2) commercial CuO-200 mesh, (3) conventional CuO. [c] Conversion (%) based on substrate = [1 − (concentration of substrate left after reaction/initial concentration of substrate)] × 100. [d] Selectivity (%) of product = (concentration of product/total concentration of all products) × 100. [e] Turnover of number = moles of converted substrate/mol of catalyst.

Table 2. Epoxidation of Alkenes with Copper Oxide[a]

Entry	Substrate	Epoxide	Conversion, %	Selectivity, %
1	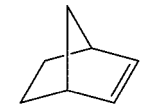	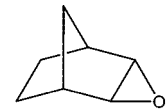	89.5	100
2	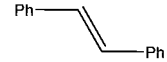	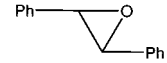	88.3	83.1
3	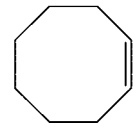	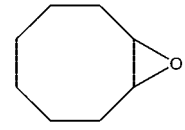	64.3	100

[a] 1 mmol alkene, 5 mmol TBHP, and 10.0 mg of CuO catalyst, stirred in 10 mL of ACN under reflux (70 °C) for 24 h.

with *t*-butylhydroperoxide as the oxidant. For comparison, CuO prepared by a conventional method and commercial available materials were also tested for epoxidation (Table 1). The epoxidation of norbornene with copper oxide prepared by our method gave 89.5% yield of norbornene epoxide, whereas the commercial CuO and the CuO prepared by the conventional method gave 78.2 and 64.3% yield, respectively. To determine the general applicability of the epoxidation process with the copper oxide catalyst, we carried out epoxidation for *trans*-stilbene and *cis*-cyclooctene and the results are summarized in Table 2. *trans*-Stilbene showed 88.3% conversion and 83% selectivity to *trans*-stilbene oxide. However, benzaldehyde, a byproduct due to the oxidative cleavage of *trans*-stilbene, was also observed. Epoxidation of *cis*-octene gave 64.3 and 100% selectivity to the corresponding epoxide.

4. Discussion

4.1. Possible Growth Mechanism of the Urchin-like CuO Materials. As shown in Figure 2, CuO shows urchin-like morphology consisting of self-assembled nanostrips. To investigate the evolution process of the urchin-like CuO, time-dependent experiments were carried out, during which

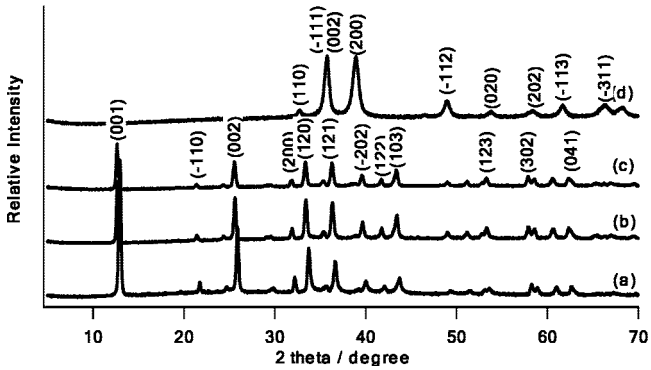

Figure 7. XRD patterns of as-collected samples at different reaction times: (a) 1, (b) 3, (c) 5, and (d) 6 h.

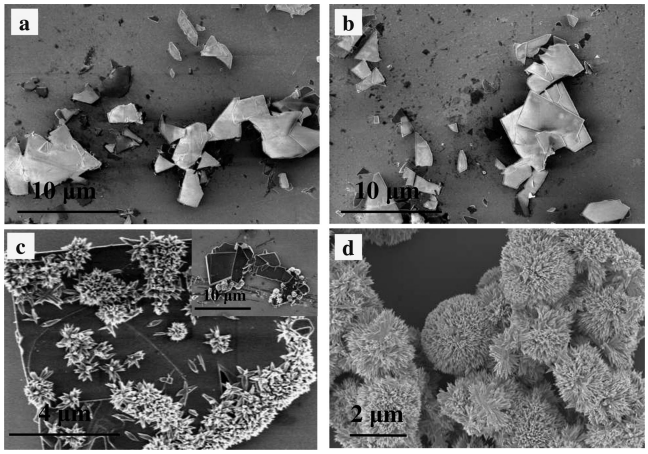

Figure 8. FE-SEM of as-collected samples at different times: (a) 1, (b) 3, (c) 5, and (d) 6 h.

the samples were collected at different times after the reflux was started. The samples were collected at 1, 3, 5, and 6 h, respectively. XRD and FE-SEM experiments were used to study the evolution of phase formation and morphologies. XRD patterns of the as-collected samples at different times are shown in Figure 7. The sample collected from 1 to 5 h showed different phases from the final product. When the reaction time was less than 5 h, the XRD patterns of the samples corresponded to copper nitrate hydroxide (JCPDS: 15−0014). When the reaction proceeded for 6 h, the product formed was CuO. The products obtained at 1−3 h had a platelike morphology, as shown in images a and b in Figure 8.

$$H_2NCONH_2(S) + H_2O(I) \xrightarrow{\Delta} CO_2(g) + NH_4^+(aq) + OH^-(aq) + NCO^-(aq) \quad (1)$$

$$[Cu(H_2O)_4]^{2+}(aq) + NO_3^-(aq) + OH^-(aq) \rightarrow Cu_2(OH)_3(NO_3)\downarrow \quad (2)$$

$$Cu_2(OH)_3(NO_3)(s) \xrightarrow[\text{excess } NH_4^+]{100\ ^\circ C} CuO(s) + [Cu(NH_3)_4]^{2+}(aq) + NO_3^-(aq) + H_2O(1) \quad (3)$$

With the extension of the reaction time to 5 h, the morphology of the products was a mixture of platelike and strips, as shown in Figure 8c. On the basis of the results from XRD, CuO was formed from the decomposition of copper nitrate hydroxide, which had a platelike morphology. The formation of CuO followed the processes, shown in eqs 1−3. Hydroxyl groups were generated from the hydrolysis of urea at a certain temperature.[11] Copper hydrate ions reacted with hydroxyl in the presence of nitrate ions to form a copper nitrate hydroxide precipitation. With the hydrolysis of urea, more and more ammonium hydroxide was produced, as mentioned in the literature.[39] Copper nitrate hydroxide converted to hydroxide when heating with a small amount of ammonium hydroxide which then underwent dehydration to the oxide. The formation of copper oxide with the intermediate of copper nitrate hydroxide in this paper is different from all of the processes for producing CuO reported in the literature.[1,4,6,9,24]

On the basis of phase formation, the evolution of morphology is discussed, as shown in Figure 8. Urchin-like morphology consisted of aggregation of strips, and the strips were from the platelike morphology. Copper nitrate hydroxide has a layer structure with a double layered intercalated nitrate ion. The nitrate ions would be squeezed out and the layer structure would collapse when dehydration occurs. The structural collapse caused the plate to break into strips, which were single crystals. The strips aggregated through oriented attachment to form the urchin-like morphology, as shown in Figure 3b. The strips are uniquely produced from the breakage of plate-like morphology, which is different from the direct growth of strips from nuclei.[6]

Time-dependent experiments showed that it is more likely that CuO was produced via the decomposition of copper nitrate hydroxide. However, the investigation of dissolution/recrystallization will be done in future studies.

4.2. Effects of Copper Sources and Precipitators on the Crystal Phase and Morphology. To investigate which factors played critical roles in the synthesis of urchin-like CuO, a variety of copper sources and precipitators were used. In these experiments, copper chloride and copper sulfate were used as copper sources instead of copper nitrate.

Figure 9 displays the powder XRD patterns of the samples prepared from different copper sources. When copper sulfate was used as the copper source, copper sulfate hydroxide was obtained. The peaks in Figure 9b indicated the formation of basic copper sulfate, which has the formula $Cu(SO_4)(OH)_4$ (JCPDS card: 07−0407). There were no CuO peaks observed. When copper chloride was used instead of copper nitrate, basic copper chloride was formed rather than copper oxide.[40] All of the reflections of the as-synthesized basic copper chloride could be assigned to orthorhombic atacamite (JCPDS: 25−0269) and rhombohedral paratacamit (JCPDS: 25−1427). The main peaks are labeled, as shown in Figure 8c, in which P represented paratacamite and A atacamite.

Figures 2and 10 show the FE-SEM images of the samples prepared from different copper sources. The copper sulfate hydroxide synthesized from copper sulfate showed rodlike

(39) Tanaka, J.; Suib, S. L. *Experimental Methods in Inorganic Chemistry*; Prentice-Hall: Upper Saddle River, NJ, 1999.
(40) Lee, S. C.; Park, S. H.; Lee, S. M.; Lee, J. B.; Kim, H. J. *Catal. Today* **2007**, *120*, 358.

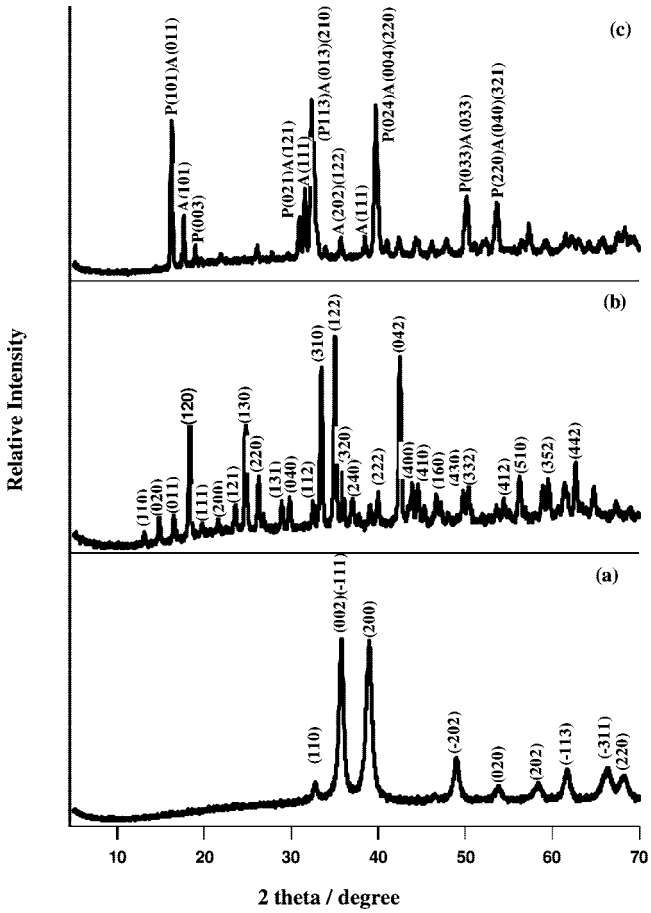

Figure 9. XRD patterns of the samples obtained with different copper sources: (a) copper nitrate, (b) copper sulfate, (c) copper chloride.

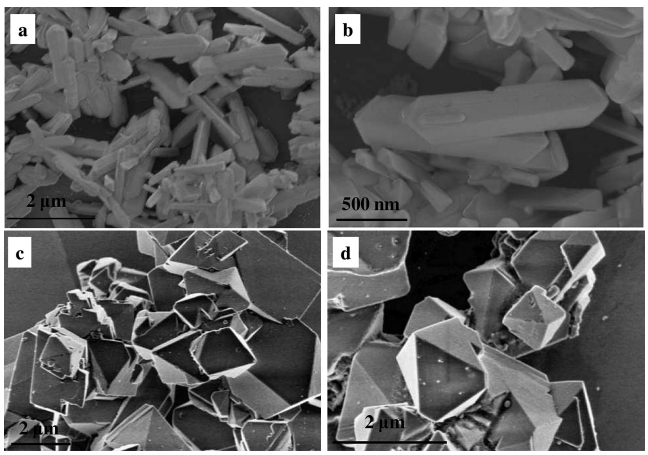

Figure 10. FE-SEM of the samples obtained with different copper sources: (a, b) copper sulfate, (c, d) copper chloride.

morphologies with various sizes. The rods had a tetragonal shape. The copper chloride hydroxide showed an octahedral morphology. They were different from the urchin-like CuO.

On the basis of the XRD results and FE-SEM images, the copper sources played very important roles in the preparation of urchin-like CuO. From the above discussion of the growth mechanism of urchin-like CuO, copper nitrate hydroxide was an intermediate in the formation of CuO. Copper nitrate hydroxide could decompose into CuO, rather than copper sulfate hydroxide and copper chloride hydroxide. We discussed why different starting copper salts yielded different products based on thermal stability of the basic copper salts.

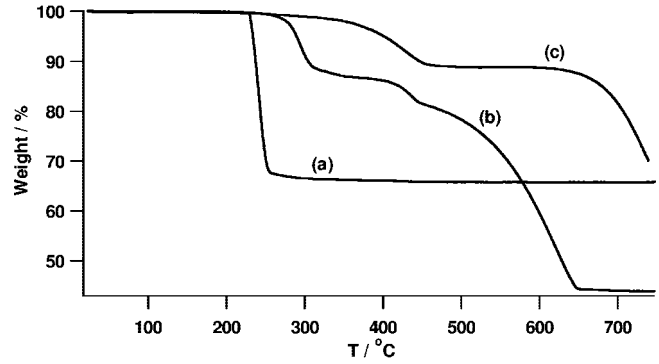

Figure 11. TGA of (a) copper nitrate hydroxide, (b) copper chloride hydroxide, and (c) copper sulfate hydroxide.

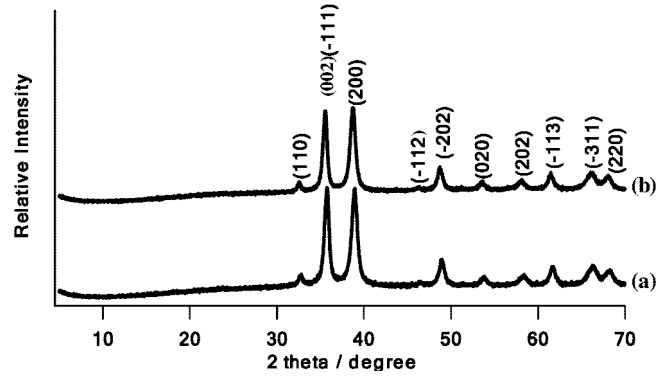

Figure 12. XRD patterns of the samples prepared with different precipitators: (a) urea, (b) ammonium hydroxide.

TGA was used to study the thermal stability of the product from different starting materials. Copper chloride hydroxide and copper sulfate hydroxide showed higher thermal stability than copper nitrate hydroxide, as shown in Figure 11. The decomposition temperatures of copper nitrate hydroxide, copper chloride hydroxide and copper sulfate hydroxide are 230, 300, and 350 °C. In addition, the same final product, CuO, was obtained at 250, 650, and 750 °C, respectively. TGA data explained why CuO was synthesized when the starting material is copper nitrate, but not copper chloride or copper sulfate.

The nature of the precipitating agent had a large influence on the properties of the eventual product.[11] In this work, the effects of precipitators were investigated. Ammonia was used in place of urea, whereas other conditions were kept the same. XRD patterns in Figure 12 show that CuO was obtained both with urea or ammonia as precipitators. As shown in Figure 13, CuO prepared in the ammonia system also showed a flowerlike morphology with different size particles. Compared to an urchin-like morphology in Figure 2, flowerlike CuO showed less homogeneity, which was caused by the nature of urea and ammonia. When urea was used, hydroxyl groups were gradually generated. With the extension of the reaction, excess ammonia led to the decomposition of copper nitrate hydroxide. In the ammonia system, CuO was generated immediately, once ammonia was added to the solution. The nucleation and crystal growth were fast, which caused the morphology to be less homogeneous.

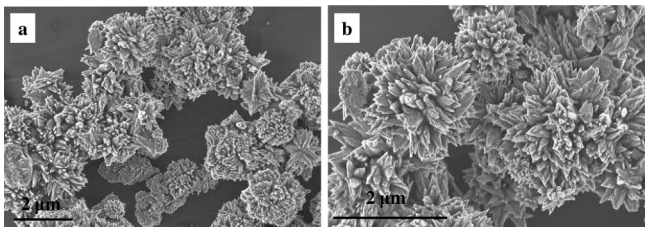

Figure 13. FE-SEM of the samples prepared with ammonium hydroxide as the precipitator.

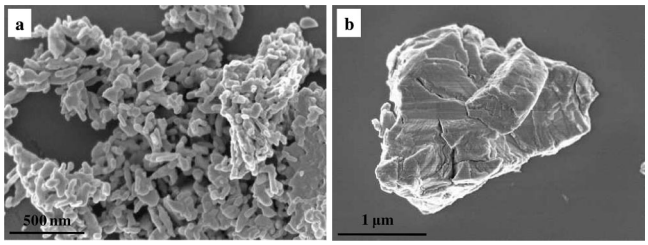

Figure 14. FE-SEM images of (a) CuO prepared by a conventional method and (b) commercially available CuO.

4.3. Catalytic Performance. Copper-based heterogeneous and homogeneous catalysts have been extensively used for chemical synthesis.[41] Nevertheless, heterogeneous catalysts are desirable over homogeneous catalysts because of their reusability and generation of less waste. The synthesized urchinlike CuO showed excellent catalytic activity for the epoxidation of alkenes. The microstructure study might help to understand the difference in catalytic performance. FE-SEM images of CuO prepared by a conventional method and commercial available CuO are shown in Figure 14. CuO prepared by a conventional method consisted of cluster of particles, however, the commercial CuO is a bulk material and has no specific shape. Therefore, the enhanced catalytic activity of the urchin-like CuO may be associated with the uniform and organized microstructure. Epoxidation of norbornene over vanadium-substituted phosphomolybdic acid catalysts has been reported recently with conversions of only 25−70%.[42] Minkata et al. have successfully carried out Cu(II) catalyzed epoxidation *trans*-stilbene using oxygen in comparable yields; however, the reactions needed extended times (48 h).[42] In the catalytic epoxidation of alkenes, the catalytic oxygen activation process uses a metal catalyst and an oxygen donor to form either a peroxo-metal or an oxo-metal intermediate.[42] In the peroxo-metal pathway, the oxidation state of the metal remains constant and the metal ion merely acts as a Lewis acid to promote the oxidizing ability of the peroxo group. The oxo-metal pathway on the other hand, involves a two-electron reduction of the metal ion, which is then reoxidized by the oxygen donor. The epoxidation of alkenes with CuO catalysts is believed to proceed via the peroxo-metal pathway. Therefore, in the epoxidation of alkenes, TBHP functions as the oxygen donor and the CuO metal catalyst act as a Lewis acid. However, detailed investigation of the mechanism of CuO catalyzed epoxidation is underway.

5. Conclusion

The facile reflux method is an effective method for the preparation of CuO, and the yield of CuO is 95%. The as-synthesized CuO had a uniform urchin-like shape composed of aggregates of the single-crystal strips. Urchin-like CuO exhibited good olefin epoxidation catalytic activity and high yield of norbornene (89.5%), compared with conventional CuO (64.3%) and commercial samples (78.2%). In the process of preparing pure phase and urchin-like CuO, both copper sources and precipitators played crucial roles, in which nitrate ion was very important because of the decomposition of copper nitrate hydroxide.

Acknowledgment. We thank the U.S. Department of Energy, Office of Basic Energy Sciences, Division of Chemical Sciences, Geosciences, and Biological Sciences, for support of this work. We thank Dr. Jim Romanow for the help with FESEM experiments in the Physiology and Neurobiology Department. We acknowledge Dr. Francis S. Galasso for helpful discussions.

CM802915M

(41) Evano, G.; Blanchard, N.; Toumi, M. *Chem. Rev.* **2008**, *108*, 3054.

(42) Moro-oka, Y. *Catal. Today* **1998**, *45*, 3.